

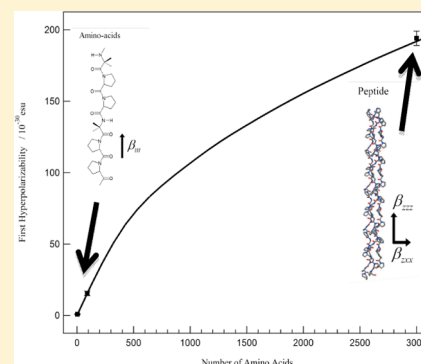
# A Bottom-Up Approach to Build the Hyperpolarizability of Peptides and Proteins from their Amino Acids

Julien Duboisset,<sup>†</sup> Ariane Deniset-Besseau,<sup>‡</sup> Emmanuel Benichou,<sup>†</sup> Isabelle Russier-Antoine,<sup>†</sup> Noelle Lascoux,<sup>†</sup> Christian Jonin,<sup>†</sup> François Hache,<sup>‡</sup> Marie-Claire Schanne-Klein,<sup>‡</sup> and Pierre-François Brevet<sup>\*,†</sup>

<sup>†</sup>Institut Lumière Matière, UMR CNRS 5306, Université Claude Bernard Lyon 1, 69622 Villeurbanne, France

<sup>‡</sup>Laboratoire d'Optique et Biosciences, Ecole Polytechnique, UMR CNRS 7645 and INSERM U696, 91128 Palaiseau, France

**ABSTRACT:** We experimentally demonstrate that some peptides and proteins lend themselves to an elementary analysis where their first hyperpolarizability can be decomposed into the coherent superposition of the first hyperpolarizability of their elementary units. We then show that those elementary units can be associated with the amino acids themselves in the case of nonaromatic amino acids and nonresonant second harmonic generation. As a case study, this work investigates the experimentally determined first hyperpolarizability of rat tail Type I collagen and compares it to that of the shorter peptide [(PPG)<sub>10</sub>]<sub>3</sub>, where P and G are the one-letter code for Proline and Glycine, respectively, and that of the triamino acid peptides PPG and GGG. An absolute value of  $(0.16 \pm 0.01) \times 10^{-30}$  esu for the first hyperpolarizability of nonaromatic amino acids is then obtained by using the newly defined  $0.087 \times 10^{-30}$  esu reference value for water. By using a collagen like model, the microscopic hyperpolarizability along the peptide bond can be evaluated at  $(0.7 \pm 0.1) \times 10^{-30}$  esu.



## INTRODUCTION

Peptides and proteins are essential elements of living bodies. They are built from the repetition of a reduced set of elementary bricks, the 20 standard naturally occurring amino acids, in a specific three-dimensional spatial organization largely determining their biological activity. Many different techniques have been used in the past to investigate their structure and their activity, e.g. X-ray spectroscopy for their spatial structure,<sup>1</sup> but there has also been a rapid development in standard optical methods like absorption, fluorescence or circular dichroism for instance.<sup>2</sup> Multiphoton microscopy has also received much attention recently because it has been immediately recognized that an intrinsic three-dimensional spatial resolution could be obtained owing to the high peak power densities required for nonlinear processes. Besides, it is a robust technique in scattering media such as biological tissues.<sup>3</sup> Further developments have been introduced to improve the tissue contrast by using a better control of the nonlinear light-matter interaction with a combination of techniques like Two Photon Excited Fluorescence (TPEF) and Second or Third Harmonic Generation (SHG or THG).<sup>4,5</sup> Nowadays, TPEF, SHG, or THG are routinely used in many laboratories throughout the world for bioimaging in particular. While nonlinear optical probes targeting specific biological tissues or specific biological activities are still highly desired, in particular for TPEF,<sup>6,7</sup> many biological tissues develop an intrinsic optical response in the absence of molecular probe. This is the case for collagen for instance.<sup>8–10</sup> Several problems must still be addressed, however, in order to eventually achieve a quantitative analysis

of the optical signals recorded, especially in the case of tissue imaging. In particular, the exact relationship between the intensity of the SHG signals and the nature of the tissues has remained elusive up to now.

In the case of SHG, we have recently undertaken a thorough investigation of the recorded intensities and their relationship with the different nonlinear optical sources found in proteins and peptides for this process. This bottom-up approach is based on the use of the technique of Hyper Rayleigh Scattering (HRS), the incoherent nonlinear scattering of light by an isotropic liquid solution.<sup>11</sup> With the design of a highly sensitive experimental setup, reaching the sensitivity of a single 80 nm diameter gold metallic particle in the sampled volume,<sup>12</sup> we have been able to measure the first hyperpolarizability, namely the efficiency of the compounds to scatter light at the second harmonic frequency, of several amino acids. In particular, we have recently investigated the aromatic amino acids Tryptophan (standard one-letter code W) and Tyrosine (one-letter code Y), have been able to give a higher limit for that of the nonaromatic one Lysine (one-letter code K), and discussed the first hyperpolarizability of the tripeptide KWK.<sup>13</sup> The main experimental difficulty encountered in these works lies in the detection of very weak signals. The direct measurement of single amino acids remains extremely difficult with the current experimental resources available. In another work, we have

Received: December 20, 2012

Revised: July 19, 2013

Published: July 23, 2013

investigated the case of rat tail Type I collagen and the shorter peptide  $[(\text{PPG})_{10}]_3$  where G is the one-letter code for Glycine and P that for Proline.<sup>14</sup> In that study, we have been able to show that it is possible to build the first hyperpolarizability of collagen from its constituting elementary units. However, this previous work could neither conclude definitively the absolute hyperpolarizability of a single amino acid nor the exact nature of the elementary units. In the present work, we address this problem, provide a value to these elementary bricks, and discuss their identification with the amino acid themselves.

**Nonlinear Optical Apparatus.** The experimental HRS setup was based on a mode-locked Ti:Sapphire laser tuned to 784 nm and delivering pulses of about 180 fs at a repetition rate of 76 MHz. The average output power was about 700 mW right after the laser exit. The fundamental beam was focused into a fused-silica cell with a microscope objective ( $\times 16$ , NA 0.32) and a red filter was placed before it to remove any residual light generated at the harmonic frequency prior to the cell. The harmonic light collection was performed at a right angle with a 25 mm focal length lens. A blue filter was placed after this collection lens to remove the fundamental light before the monochromator entrance. A water-cooled photomultiplier tube was used to detect the SH photons. No polarization selection was made on the harmonic beam to favor the sensitivity of the experimental system owing to the low level of the signal intensity. The fundamental beam was chopped at 130 Hz to enable a gated photon counting regime and remove the background photons. The monochromaticity of the second harmonic light generated was always assessed prior to further experiments to reject any spurious contribution from fluorescence. Preliminary experiments were also performed on the solvent in absence of amino acids for reference measurements.

**Chemicals.** GGG and PPG triamino acids were purchased from Sigma-Aldrich and used as received. Ultra pure water purified with a Millipore filtering system (Bedford, MA) with a resistivity of 18.2 M $\Omega$ -cm was used throughout.

## RESULTS AND DISCUSSION

Rat tail Type I collagen is recognized for yielding large signals in SHG microscopy, a property arising from the non-centrosymmetric molecular structure of the protein, see Figure 1. Rat tail Type I collagen is a rigid rod-like protein formed by a 290 nm long helix composed of three interwoven  $\alpha$  chains. The primary sequence of the three  $\alpha$  chains is the repetition of the motif  $\text{GX}_1\text{X}_2$ , with  $\text{X}_1$  and  $\text{X}_2$  corresponding mainly to proline and hydroxyproline. However, none of those two amino acids G and P are expected to possess a strong first hyperpolarizability because they do not possess an extended delocalized  $\pi$ -electron system in a noncentrosymmetric environment. To understand the origin of the strong efficiency of Type I collagen for SHG, we have recently reported the experimental measurement of the first hyperpolarizability of the rat tail Type I collagen for an excitation wavelength of 790 nm. Since Type I collagen does not present any resonance in the visible range of the spectrum, the excitation wavelength was not critical apart from its comparison to the 290 nm length of the Type I collagen triple helix. The first hyperpolarizability of Type I collagen was found to be  $(1250 \pm 20) \times 10^{-30}$  esu, using the value of  $0.56 \times 10^{-30}$  esu for the first hyperpolarizability of the acetic acid buffer solution as a reference.<sup>14</sup> However, this reference value has been shown recently to be overestimated and should better read as  $0.087 \times 10^{-30}$  esu.<sup>13,15</sup>

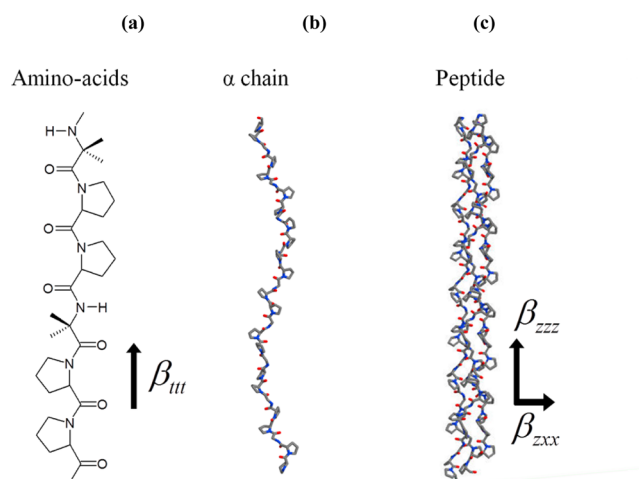


**Figure 1.** Schematics of rat tail Type I collagen structure: (a) amino acid sequence and (b)  $\alpha$  chain and (c) collagen rods.

Using this newly defined reference value, the first hyperpolarizability of Type I collagen is  $(188 \pm 3) \times 10^{-30}$  esu. In a similar way, the first hyperpolarizability of the short peptide  $[(\text{PPG})_{10}]_3$ , only 8.6 nm long and with the similar spatial structure, was also measured and found to be  $(99 \pm 6) \times 10^{-30}$  esu with  $0.56 \times 10^{-30}$  esu as a buffer solution reference or  $(14.9 \pm 0.9) \times 10^{-30}$  esu with the refined reference value of  $0.087 \times 10^{-30}$  esu, using the same buffer solution reference. These results were found consistent with the three-dimensional structural model for rat tail Type I collagen taking into account the rod-like shape of the protein, its incorporation of three interwoven  $\alpha$  chains, and its primary sequence. The model assumed a coherent summation of the response of single units over the whole protein. Because the length of Type I collagen is not negligible compared to the optical wavelength, the model also took into account the retardation of the exciting and harmonic generated fields over the length of the collagen rod. Within this framework, it appeared that the first hyperpolarizability of Type I collagen and of the  $[(\text{PPG})_{10}]_3$  peptide could be rationalized by starting from the first hyperpolarizability of elementary units, provided corrections were made for the length of the structure. However, no direct conclusions could be made on the exact nature of the elementary bricks introduced with this model.

To address this unsolved question, we have thus performed further experiments to measure the first hyperpolarizability of single PPG motifs. However, the HRS intensity was rather small and it was difficult to follow the standard protocol involving the construction of dilution plots. We proceeded instead with the recording of the HRS intensity for long periods of time in order to obtain counting errors much smaller than the difference in intensity recorded for the two samples, namely with and without PPG. Figure 2 reports the scan of the harmonic wavelength over the HRS band for a fixed fundamental wavelength of 784 nm. The difference in intensity is larger than the error bars when the counting period reaches at least 100 s. By using the PPG concentration of the solution, the first hyperpolarizability was found to be  $(0.75 \pm 0.06) \times 10^{-30}$  esu by using the newly defined solvent reference of  $0.087 \times 10^{-30}$  esu.<sup>14</sup> Hence, despite the absence of any strongly delocalized  $\pi$ -electrons, a detectable signal was observed and a first hyperpolarizability measured for the PPG motif. By using a

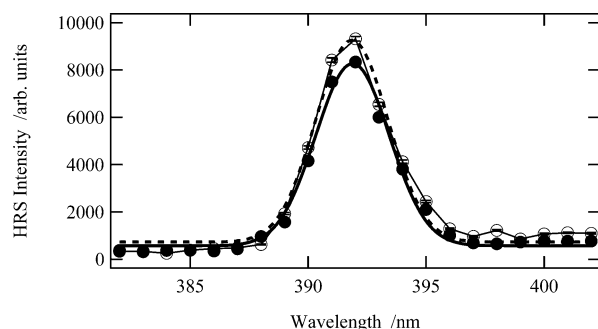


**Figure 2.** HRS intensity recorded as a function of the wavelength for a fixed fundamental wavelength of 784 nm for (filled disks) the neat water solvent and (empty disks) a GPP aqueous solution. Error bars have the size of the markers or smaller.

similar procedure, the first hyperpolarizability of a single GGG motif was found to be  $(0.90 \pm 0.3) \times 10^{-30}$  esu, in the same range of magnitude as that of PPG. Interestingly, that of Lysine (K) was reported in an earlier work and an upper limit was measured to be  $0.23 \times 10^{-30}$  esu.<sup>13</sup> The first hyperpolarizability of a single Glycine or Proline could not be measured, however, for sensitivity reasons. Lysine was only accessible to such a measurement owing to its much larger solubility. For comparison, Tryptophan or Tyrosine, two aromatic amino acids, have been found to have a first hyperpolarizability about ten times as large as that of a single nonaromatic amino acid in nonresonant conditions.<sup>13</sup>

The coherent model developed for Type I collagen was then extrapolated down to small peptides. Figure 3 gives a summary of the results. It displays the experimentally measured first hyperpolarizabilities as a function of the number of amino acids. The four points displayed correspond to the experimental cases studied: PPG and GGG ( $n = 3$  amino acids),  $[(PPG)_{10}]_3$  ( $n = 90$ ) and rat-tail Type I collagen ( $n = 3033$ ). For the smallest peptides, the length of the rod-like peptide is negligible

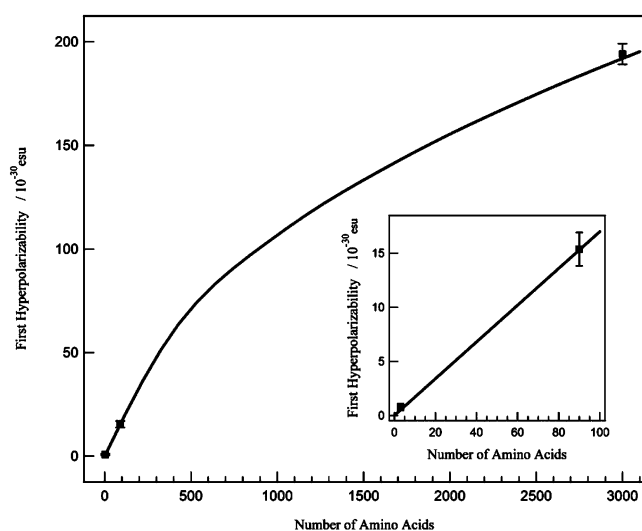


**Figure 3.** Coherent structural model for Type I collagen yielding the first hyperpolarizability as a function of the number of amino acids considered. The filled squares are the experimental values obtained for PPG and GGG ( $n = 3$ ),  $[(PPG)_{10}]_3$  ( $n = 90$ ), and rat-tail Type I collagen ( $n = 3033$ ). The solid line corresponds to fitting with the coherent model. Insert: Close-up view of the linear behavior of the structural model at low amino acid numbers.

compared to the optical wavelength and the first hyperpolarizability scales linearly with the number of amino acids present in the sequence, as one can check with the inset of Figure 3. On the other hand, for the rat-tail Type I collagen whose length is comparable to the optical wavelength, retardation effects must be taken into account,<sup>14</sup> resulting in the observed bend in Figure 3. Adjustment with our model provides a value of  $(0.16 \pm 0.01) \times 10^{-30}$  esu for a single elementary unit in the macroscopic frame, using the newly defined reference.

This value is in good agreement with the one previously reported.<sup>16</sup> The first hyperpolarizability of a single monomer peptide unit was estimated to be about  $(2 \pm 1) \times 10^{-31}$  esu from electric field induced SHG experiments (EFISHG) on the poly- $\gamma$ -benzyl-L-glutamate (PBLG) polypeptide at the fundamental wavelength of 1064 nm. It is interesting to notice that both GGG and PPG have the same hyperpolarizability. This seems to indicate that for nonaromatic amino acids, the origin of the first hyperpolarizability lies in the peptide bond rather than in the pending chains. It is also important to note that the above value would really correspond to the contribution of a unique peptide bond if the various amino acids were perfectly aligned in the peptide. Actually, it is not the case and this value rather corresponds to the average projection of the hyperpolarizability tensor on the peptide direction.

This correction may be estimated by taking into account complementary measurements of the depolarization ratio  $D$  from polarization-resolved HRS experiments. This measurement was performed with  $[(PPG)_{10}]_3$ , which exhibits enough HRS intensity to enable selection of a defined light polarization configuration. A depolarization ratio of  $D = 0.115$  was obtained.<sup>14</sup> Assuming a cylindrical symmetry as suggested by the peptide geometry, the measured value of the first hyperpolarizability then reads:

$$\beta^2 = \beta_{XXX}^2 + \beta_{ZZX}^2 = \beta_{XXX}^2(1 + D) \quad (1)$$

where  $\beta_{XXX}$  in the laboratory frame is obtained from  $\beta_{zzz}$  and  $\beta_{zzx}$  in the microscopic frame of the peptide as follows:<sup>17</sup>

$$\beta_{XXX}^2 = \frac{1}{7}\beta_{zzz}^2 + \frac{12}{35}\beta_{zzz}\beta_{zzx} + \frac{24}{35}\beta_{zzx}^2 \quad (2)$$

where  $z$  is taken along the peptide axis and  $x$  perpendicularly to it whereas  $X$  is the vertical laboratory direction perpendicular to the  $Z$  propagation direction of the exciting fundamental light beam. To go further in our approach, we have to make some assumptions about the nature of the elementary bricks exhibiting a nonlinear response in the triple helix. Hence, we assume that this elementary brick is the peptide bond and that it behaves as a rod-like entity with a nonvanishing nonlinear optical response along the bond direction  $t$ . This effective elementary brick first hyperpolarizability  $\beta_{ttt}$  represents the mean response of a peptide bond in a triple helical environment, although the nonlinear response of peptide bonds in another peptide may be more complex.<sup>18</sup> The hyperpolarizability components in the microscopic frame then read:

$$\begin{aligned} \beta_{zzz} &= n\langle(\hat{z} \cdot \hat{t})^3\rangle\beta_{ttt} \\ \beta_{zzx} &= n\langle(\hat{z} \cdot \hat{t})(\hat{x} \cdot \hat{t})^2\rangle\beta_{ttt} \end{aligned} \quad (3)$$

where  $\hat{z}$ ,  $\hat{x}$ , and  $\hat{t}$  are the unit vectors of the different frames, with the  $z$  axis long the triple helix main axis, the broken



brackets stand for the orientational averaging, and  $n$  is the number of amino acids. This approach implies that the Kleimann symmetry is satisfied. Accordingly, we have verified that the collagen and the peptide solutions show very weak optical absorbances at the fundamental and harmonic wavelengths. Note, however, that the validity of Kleinmann symmetry in collagen is still an open question.<sup>19,20</sup>

In eq 3, one may consider the geometry of the collagen-like peptide [(PPG)<sub>10</sub>]<sub>3</sub> and assume a pitch angle of 45° for the orientational averaging (see Figure 1), which results in a ratio  $\rho = \beta_{zzz}/\beta_{zzx} = 2$ . Alternatively, one may use the value  $\rho = \beta_{zzz}/\beta_{zzx} = 1.4$  that has been measured in collagen-rich tissues<sup>20</sup> and corresponds to an effective pitch angle of 50° of the elementary brick nonlinear dipole. Moreover, the latter value is in good agreement with theoretical calculations that consider a more complex nonlinear response at the peptide bond scale.<sup>18</sup> Finally, combining eqs 1 to 3:

$$\beta_{\text{eff}} = \frac{\beta}{\sqrt{n^2(1 + D)G}} \quad (4)$$

where the geometrical factor  $G$  reads as:

$$G = \frac{1}{7} \langle (\hat{z} \cdot \hat{t})^3 \rangle^2 + \frac{12}{35} \langle (\hat{z} \cdot \hat{t})^3 \rangle \langle (\hat{z} \cdot \hat{t})(\hat{x} \cdot \hat{t})^2 \rangle + \frac{24}{35} \langle (\hat{z} \cdot \hat{t})(\hat{x} \cdot \hat{t})^2 \rangle^2 \quad (5)$$

Numerically,  $\beta_{\text{eff}}$  is then evaluated as  $(0.6 \pm 0.1) \times 10^{-30}$  esu assuming a pitch angle of 45° ( $\rho = 2$ ), or as  $(0.7 \pm 0.1) \times 10^{-30}$  esu assuming an effective pitch angle of 50° ( $\rho = 1.4$ ). Although it requires an assumption on the geometry of the peptide and the nature of the elementary brick to introduce the nonlinear response, this calculation further supports the case for an elementary brick responsible for the response of collagen taken as the peptide bond itself in each individual amino acid.

To further rationalize the collagen model and the present results, one can also compare the first hyperpolarizability of denatured collagen with the present results. It has been found that rat tail Type I collagen submitted to thermal denaturation at 50 °C for 10 min has a first hyperpolarizability of  $(25 \pm 3) \times 10^{-30}$  esu for a single  $\alpha$  chain formed from 337 amino acids.<sup>14</sup> This value is 7.5 times smaller than the first hyperpolarizability of nondenatured collagen, the value of which is  $188 \times 10^{-30}$  esu. This is a much smaller value than expected from the three interwoven  $\alpha$  chains structure of collagen. Hence, it was assumed that some degree of disorder was present in the denatured collagen, the single  $\alpha$  chains having a tendency to organize themselves into random coils. A complete randomness of the spatial distribution of the amino acids forming the  $\alpha$  chains should lead to a square-root dependence of the first hyperpolarizability with the number of amino acids. Indeed, the response from a random coil should be very similar to that of a solution of the same number of randomly oriented amino acids. This dependence arises from the linear dependence of the HRS intensity itself with the number of the scattering units, hence the square root when going down to the hyperpolarizability level. Therefore, the first hyperpolarizability of a denatured collagen  $\alpha$  chain where the amino acids are randomly oriented should be of the order of  $\sqrt{n}\beta_0 = 5.5 \times 10^{-30}$  esu, where  $n$  is the number of amino acids and  $\beta_0$  the hyperpolarizability of a single amino acid. On the other hand, the fully coherent superposition of an extended 337 amino acid  $\alpha$  chain is about  $63 \times 10^{-30}$  esu, as determined by the simple ratio of the first

hyperpolarizability of nondenatured collagen and the number of  $\alpha$  chains forming the protein. The experimentally determined value of  $25 \times 10^{-30}$  esu indicates therefore that, to a large extent, spatial order is still present in denatured collagen, at least when using short time thermal denaturation. Random coils of single  $\alpha$  chains from denatured collagen cannot therefore be assimilated to fully random distributions of their constituents. Single  $\alpha$  chains must preserve some stiffness preventing complete disordering.

## CONCLUSIONS

This work constitutes a first step in linking the microscopic first hyperpolarizability of nonaromatic amino acids taken as elementary bricks with that of peptides and proteins. In the case of rat tail Type I collagen, the elementary bricks are associated with the Glycine and Proline amino acids and their first hyperpolarizability is measured. Interestingly, at the level of sensitivity of the present measurements, it is not possible to distinguish the different amino acids from the value of their first hyperpolarizability. This result suggests that their origin possibly lies in the peptide bond itself. This hyperpolarizability remains nevertheless much smaller than that of the aromatic amino acids like Tryptophan and Tyrosine in nonresonant conditions. Several questions remain, though. One concerns the generality of the present concepts to build the first hyperpolarizability of proteins from their constituting amino acids. It is indeed not expected that aromatic amino acids like Tryptophan and Tyrosine, or nonaromatic amino acids with larger residues, lend themselves to a similar behavior owing to stronger interactions depending on their spatial organization. Considering that all nonaromatic amino acids investigated in this study exhibit a similar hyperpolarizability within our measurements sensitivity, we tentatively attribute the nonlinear response of nonaromatic amino acids to the peptide bond itself. Advanced theoretical calculations should help to address this question. This task has already been undertaken for (PPG)<sub>10</sub> where an additive model has been used in combination with TDDFT calculations, using *N*-methylacetamide as a model for the peptide bond.<sup>21</sup> The model does not implement field retardation, unnecessary considering the length of the peptide.<sup>22</sup> Our results are in agreement with this work. Another study has been performed recently about Type I collagen showing rather good agreement with our data.<sup>18</sup> Further studies must, however, be considered along those lines for other proteins and amino acids in order to formulate more general rules.

## AUTHOR INFORMATION

### Corresponding Author

\*Tel: +33 (0)472 44 58 73. Fax: +33 (0)472 44 58 71. E-mail: pfbrevet@univ-lyon1.fr.

### Notes

The authors declare no competing financial interest.

## ACKNOWLEDGMENTS

J.B., E.B., I.R.A., Ch.J., N.L., and P.F.B. thank the Region Rhône-Alpes for financial support through a CIBLE grant. A.D.-B. thanks the Fondation de la Recherche Médicale for financial support.

## ■ REFERENCES

- (1) Petsko, G. A.; Ringe, D. Fluctuations in Protein Structure from X-ray Diffraction. *Annu. Rev. Biophys. Bioeng.* **1984**, *13*, 331–371.
- (2) Schmid, F. X. In *Protein Structure, A Practical Approach*; Creighton, T. E., Ed.; Oxford University Press: London, UK, 1997; Chapter 11.
- (3) Denk, W.; Strickler, J. H.; Webb, W. W. Two Photon Laser Scanning Fluorescence Microscopy. *Science* **1990**, *248*, 73–76.
- (4) Moreaux, L.; Sandre, O.; Mertz, J. Membrane Imaging by Second Harmonic Generation Microscopy. *J. Opt. Soc. Am. B* **2000**, *17*, 1685–1694.
- (5) Débarre, D.; Supatto, W.; Beaufrepaire, E. Structure Sensitivity in Third Harmonic Generation Microscopy. *Opt. Lett.* **2005**, *30*, 2134–2136.
- (6) Albota, M. A.; Xu, C.; Webb, W. W. Two-Photon Fluorescence Excitation Cross Sections of Biomolecular Probes from 690 to 960 nm. *Appl. Opt.* **1998**, *37*, 7352–7356.
- (7) Campagnola, P. J.; Loew, L. M. Second Harmonic Imaging Microscopy for Visualizing Biomolecular Arrays in Cells, Tissues and Organisms. *Nat. Biotechnol.* **2003**, *21*, 1356–1360.
- (8) Mohler, W.; Millard, A. C.; Campagnola, P. J. Second Harmonic Generation Imaging of Endogenous Structural Proteins. *Methods* **2003**, *29*, 97–109.
- (9) Freund, I.; Deutsch, M.; Sprecher, A. Connective Tissue Polarity. Optical Second-Harmonic Microscopy, Crossed-Beam Summation, and Small-Angle Scattering in Rat-Tail Tendon. *Biophys. J.* **1986**, *50*, 693–712.
- (10) Zipfel, W. R.; Williams, R. M.; Christie, R.; Nikitin, A. Y.; Hyman, B. T.; Webb, W. W. Live Tissue Intrinsic Emission Microscopy Using Multiphoton-Excited Native Fluorescence and Second Harmonic Generation. *Proc. Natl. Acad. Sci. U.S.A.* **2003**, *100*, 7075–7080.
- (11) Clays, K.; Persoons, A. Hyper-Rayleigh Scattering in Solution. *Phys. Rev. Lett.* **1991**, *66*, 2980–2983.
- (12) Duboisset, J.; Russier-Antoine, I.; Benichou, E.; Bachelier, G.; Jonin, Ch.; Brevet, P. F. Single Metallic Nanoparticle Sensitivity with Hyper Rayleigh Scattering. *J. Phys. Chem. C* **2009**, *113*, 13477–13481.
- (13) Duboisset, J.; Matar, G.; Russier-Antoine, I.; Benichou, E.; Bachelier, G.; Jonin, Ch.; Ficheux, D.; Besson, F.; Brevet, P. F. First Hyperpolarizability of the Natural Aromatic Amino Acids Tryptophan, Tyrosine, and Phenylalanine and the Tripeptide Lysine-Tryptophan-Lysine Determined by Hyper-Rayleigh Scattering. *J. Phys. Chem. B* **2010**, *114*, 13861–13865.
- (14) Deniset-Besseau, A.; Duboisset, J.; Benichou, E.; Hache, F.; Brevet, P. F.; Schanne-Klein, M.-C. Measurement of the Second-Order Hyperpolarizability of the Collagen Triple Helix and Determination of its Physical Origin. *J. Phys. Chem. B* **2009**, *113*, 13437–13445.
- (15) Campo, J.; Desmet, F.; Wenseleers, W.; Goovaerts, E. Highly Sensitive Setup for Tunable Wavelength Hyper-Rayleigh Scattering with Parallel Detection and Calibration Data for Various Solvents. *Opt. Express* **2009**, *17*, 4587–4604.
- (16) Levine, B. F.; Bethea, C. G. Second Order Hyperpolarizability of a Polypeptide  $\alpha$ -Helix: Poly- $\gamma$ -Benzyl-L-Glutamate. *J. Chem. Phys.* **1976**, *65*, 1989–1993.
- (17) Brasselet, S.; Zyss, J. Multipolar Molecules and Multipolar Fields: Probing and Controlling the Tensorial Nature of Nonlinear Molecular Media. *J. Opt. Soc. Am. B* **1998**, *15*, 257–287.
- (18) Tuer, A. E.; Krouglov, S.; Prent, N.; Cisek, R.; Sandkuijl, D.; Yasufuku, K.; Wilson, B. C.; Barzda, V. Nonlinear Optical Properties of Type I Collagen Fibers Studied by Polarization Dependent Second Harmonic Generation Microscopy. *J. Phys. Chem. B* **2011**, *115*, 12759–12769.
- (19) Su, P. J.; Chen, W. L.; Chen, Y. F.; Dong, C. Y. Determination of Collagen Nanostructure from Second-Order Susceptibility Tensor Analysis. *Biophys. J.* **2011**, *100*, 2053–2062.
- (20) Tiaho, F.; Recher, G.; Rouède, D. Estimation of helical angles of myosin and collagen by second harmonic generation imaging microscopy. *Opt. Express* **2007**, *17*, 12286–12295.
- (21) Gusachenko, I.; Tran, V.; Houssen, Y. G.; Allain, J. M.; Schanne-Klein, M.-C. Polarization-Resolved Second-Harmonic Generation in Tendon upon Mechanical Stretching. *Biophys. J.* **2012**, *102*, 2220–2229.
- (22) Loison, C.; Simon, D. Additive Model for the Second Harmonic Generation Hyperpolarizability Applied to a Collagen-Mimicking Peptide (Pro-Pro-Gly)<sub>10</sub>. *J. Phys. Chem. A* **2010**, *114*, 7769–7779.
- (23) Perry, J. M.; Moad, A. J.; Begue, N. J.; Wampler, R. D.; Simpson, G. J. Electronic and Vibrational Second-Order Nonlinear Optical Properties of Protein Secondary Structural Motifs. *J. Phys. Chem. B* **2005**, *109*, 20009–20026.